Peer-reviewed version available at Materials 2019, 12, 1533; doi:10.3390/ma12091533

Article

Colorimetric detection of mercury ions in water with capped silver nanoprisms

Fouzia Tanvir [1], Atif Yaqub [1], Shazia Tanvir [2], Ran An [2] and William A. Anderson [2,*]

[1] Dept. of Zoology, Government College University, Lahore, Pakistan
[2] Dept. of Chemical Engineering, University of Waterloo, Canada
* Correspondence: wanderson@uwaterloo.ca

Abstract: The emission of mercury (II) from coal combustion and other industrial processes continues to be a concern and have local impact on water resources. The detection of these ions in water with sensitive but rapid testing methods is desirable for environmental screening and fieldwork. Nanoparticles of various chemistries have shown promise for this purpose, as they can be used in simple colorimetric analyses. Silver nanoprisms were chemically synthesized resulting in a blue reagent solution, that transitioned towards yellow and colorless solutions when exposed to Hg^{2+} ions at various concentrations. A rapid galvanic reduction of Hg^{2+} onto the nanoprism surfaces is apparently responsible for a change in shape towards spherical nanoparticles, leading to the change in color. There were no interferences by other metal ions in solution, and pH had minimal effect in the range of 6.5 to 9.8. The silver nanoprism reagent provided a detection limit of approximately 0.5 μM (100 μg/L) for mercury (II), which compares favorably with other nanoparticle-based techniques. Further optimization may reduce this detection limit.

Keywords: nanoparticles; spectral blue shift; amalgam; water quality

1. Introduction

Mercury has been emitted by various industrial processes over the past century, with artisanal gold mining and coal combustion as the two largest sources currently, at 775 and 558 Mg per year respectively [1]. For coal combustion, just under 30% of these emissions are in the divalent form [1], Hg^{2+}, which tends to have a high water solubility and shorter lifetime in the environment resulting in more local deposition [2]. As a monitoring tool, it is desirable to measure mercury content in aqueous samples to identify water sources that may be impacted by mercury emissions. The most common laboratory methods, using cold vapor atomic fluorescence spectrometry or atomic absorption spectrometry, are sensitive and accurate but require specialized facilities and equipment [3]. For screening purposes, it is desirable to have simple and rapid mercury measurement techniques that can be used in the field, even if their sensitivity, accuracy and selectivity may not be as good as laboratory instrumentation. Therefore, a number of other mercury detection methods have been developed over the years, ranging from colorimetric to electrochemical methods [4]. Examples for the detection of aqueous phase mercury (II) include a nanoparticle-functionalized carbon paper electrode [5], a gold nanoparticle-aptamer colorimetric method [6], and a gold nanozyme paper chip [7].

The use of gold and silver nanoparticles for colorimetric Hg^{2+} detection has been a focus of research in recent years [8]. Gold nanoparticles (AuNPs), functionalized or capped with various surface ligands, exhibit a spectral shift or color change when aggregated or dis-aggregated by the presence of Hg^{2+} [8]. Silver nanoparticles (AgNPs) can likewise undergo a spectral shift due to aggregation, but the reduction of Hg^{2+} by Ag oxidation is also cited as a mechanism for color change

[8], with Hg-Ag amalgams also produced in some reports. Limits of detection for the nanoparticle-based methods vary widely depending on the specific formulation and measurement method (e.g. instrumental versus visual), but they tend to fall within the range of 10 nM to 55 μM mercury for AgNPs [8].

A variety of different AgNP synthesis methods have been reported in the context of mercury detection. Biological "green" synthesis has been used to for AgNPs that shift in colour from yellow to colorless in the presence of mercury [9]. Chemically-synthesized AgNPs with a cytosine triphosphate cap, with a similar decrease in yellow colour in the presence of mercury [10]. Another chemically-synthesized AgNP with a gelatin functionalization likewise showed a color change from yellow to colorless for Hg^{2+} concentrations as low as 25 nM [11]. A different color change, from orange to yellow, was created using AgNPs aggregated by the combination of mercury and lysine [12]. Other AgNP detection methods for mercury have employed surface modifications including oligonucleotides [13], glutathione [14], and leaf extracts [15], for example, but the stability and suitability of these materials may be a limiting factor for commercial development.

The majority of reports have been based on spherical AgNPs, and the blue-shift in absorbance generally results in the disappearance of the initial yellow color. A few researchers have used non-spherical nanoparticles such as one using triangular nanoplates assembled into thin films which resulted in a blue color [16]. For visual detection, there are some advantages of having a more intense starting color such as blue, since the blue-shift caused by mercury may result in a more diverse color change across the color spectrum.

Therefore, in this work a simple chemical synthesis technique was adopted from earlier work with silver nanoprisms [17] to formulate non-spherical AgNPs with a visually-intense blue starting color. A straightforward capping method using polyvinylpyrrolidone was used to stabilize the AgNPs in solution in a form that may be commercially acceptable for shelf-life. The response of these AgNPs was tested to determine the spectral response to Hg^{2+} in water, and the sensitivity and selectivity was determined.

2. Materials and Methods

All chemicals used were of analytical grade or of the highest purity available. All solutions were prepared with ultra-pure water of typical resistivity 18.2 MΩ·cm. All chemicals were purchased from Sigma Aldrich (Canada) including sodium borohydride ($NaBH_4$, 99.99%), hydrogen peroxide (H_2O_2 30%), silver nitrate ($AgNO_3$, 99.99%), trisodium citrate dihydrate ($C_6H_5O_7Na_3$ $2H_2O$, 99.99%), HNO_3 and polyvinylpyrrolidone (PVP, Mw = 40,000), and the metal salts $CdCl_2$, $HgCl_2$, K_2CrO_4, $Pb(NO_3)_2$, $Cd(NO_3)_2$, $MgSO_4$, , $CoCl_2{\cdot}6H_2O$, $Pb(NO_3)_2$, $MnSO_4$, $CuSO_4$, $FeCl_2$, $BaCl_2$, NaCl and KCl. The stock solutions of metal ions were prepared by dissolving a known amount of salts in 100 mL deionized water and these were further diluted as necessary. All glassware was thoroughly cleaned with aqua regia and rinsed thoroughly with deionized water prior to use.

Silver nanoprisms were synthesized as follows. Sodium citrate (5.5 mM) was prepared in 100 mL deionized water, followed by adding 340 μL of $AgNO_3$ (30 mM) and 560 μL H_2O_2 (30%). Then 2.3 mL $NaBH_4$ (100 mM) was added and vigorously stirred. After 2 min, the colorless solution turned yellow and then rapidly darkened until a stable blue color was developed after 5 min. PVP was added at the final concentration of 0.03% as a capping agent to further stabilize the silver nanoprisms. The synthesized AgNPs were stored in the dark and used as a stock solution [18]. The silver nanoprism solution absorbance was set by dilution to approximately 0.6 at 665 nm for use in mercury detection.

The synthesized silver nanoprisms were characterized using UV-visible spectrophotometry (HP 8542 Diode Array, Agilent Technologies, USA), energy-dispersive spectroscopy (EDX), transmission electron microscopy (TEM), dynamic light scattering (DLS) and zeta potential. The colloidal solutions were centrifuged at 10,000 g and washed three times with deionized water. The washed samples were prepared by drying nanoparticles on a carbon tape. The elemental analysis of the nanoparticles was performed by energy dispersive X-ray (EDX) attached to the scanning electron

96 microscope (FEI/Philips XL30 FEG ESEM). The TEM samples were prepared by drop-coating the
97 aqueous solution of nanoprisms onto a carbon coated copper grid (200 mesh), followed by air-drying
98 for 2 hours. TEM characterization was performed using a Philips CM10.
99 A Zetasizer Nano ZS90 (Malvern Instruments Ltd, Malvern, UK) was used to measure particle
100 size distribution, polydispersity index, and zeta potential, using triplicate runs with 10 measurements
101 in each, and the Dispersion Technology software 5.1. For this analysis a refractive index of 1.5 was
102 used and the viscosity was assumed to be equal to that of the dispersant liquid.
103 The PVP capped nanoprisms were tested with various metal ions in aqueous solution with pH
104 ranging from 5.8 to 9.7. The pH-dependent response was tested by dissolving the previously
105 mentioned heavy metal salts in buffer (5 mM phosphate buffered saline). For the detection of Hg^{2+},
106 test solutions of different concentrations were mixed with the AgNP reagent in a 1:1 ratio in a buffer
107 solution and left at room temperature for 30 min, after which the UV−Vis absorption spectra were
108 recorded. The selectivity of the nanoparticle response to Hg^{2+} over other metal ions (Pb^{2+}, Cd^{2+}, Zn^{2+},
109 Mg^{2+}, Mn^{2+}, Ba^{2+}, Co^{2+}, Fe^{2+}, Cu^{2+}, Na^{+}, K^{+}) was investigated under the same optimized conditions. The
110 selectivity was evaluated using the absorption spectra of prismatic nanosilver with several metal ions
111 with concentrations ranging from 1 to 10 μmol/L. EDTA chelation was used as a negative control
112 to confirm the selectivity by binding with metal ions in solution. The metal ions were mixed with 10
113 mM of EDTA solution before the addition of the AgNPs.

114 **3. Results and Discussion**

115 *3.1. Characterization of the Test Material*

116 Silver nanoprisms were prepared via chemical reduction of silver nitrate. The sodium citrate and
117 hydrogen peroxide were added before $NaBH_4$, and the solution turned yellow first, but after 2
118 minutes the color had converted to blue due to a shift in the surface plasmon resonance (SPR) of the
119 metallic nanostructures. The transition from spherical silver nanoparticles to nanoprisms in this
120 approach is explained by the use of a strong reductant (sodium borohydride) to induce the reduction
121 of silver nitrate and the formation of small spherical silver nanoparticles (yellow) at room
122 temperature. Subsequently, the remaining hydrogen peroxide in the solution induces anisotropic
123 oxidation of portions of the nanoparticles into Ag^{+} ions and their concurrent transformation into
124 nanoprisms. The presence of hydrogen peroxide in combination with sodium citrate and sodium
125 borohydride is important for the synthesis of silver nanoprisms [19].
126 To verify the nature of the prepared colloidal suspension, the surface plasmon resonance (SPR)
127 peak is seen in the UV-Vis absorbance spectrum (Figure 1). The UV–Vis measurements of the
128 colloidal solution clearly reflect their anisotropic shape since it features a small shoulder at around
129 450 nm (typical for nanospheres), and a more intense band at around 665 nm which has been reported
130 previously for nanoprisms [17].
131

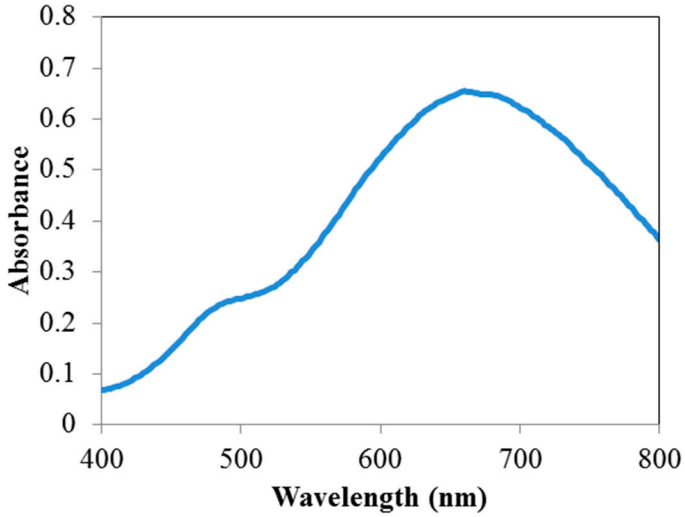

Figure 1: UV-visible spectrum of the silver colloid solution showing SPR peak around 665 nm.

This interpretation of the UV–Vis measurement agrees with the TEM analysis, where the morphology of the colloidal silver (Figure 2A) clearly confirms the presence of silver nanoprisms with most of the particles in the size range 35 ±5 nm. The particle size distribution profile has also been confirmed by DLS (Figure 2B), with an average size of 34.5 ± 6 nm, which was in good agreement with the TEM results. The polydispersity index (PDI) was lower than 0.3 in all cases, which is indicative of a monodisperse system. The particles were determined to be negatively charged with a zeta potential of −27.6 ±2 mV (Figure 3).

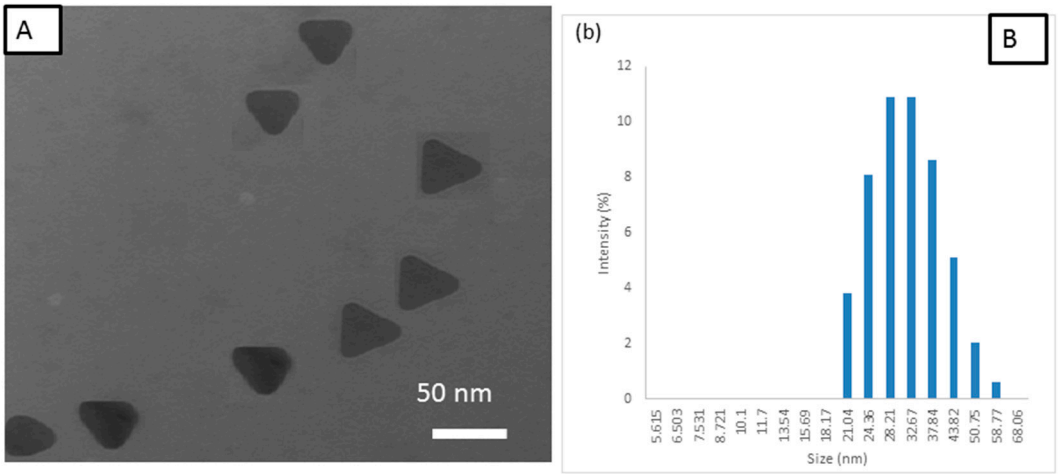

Figure 2: (A) TEM micrograph and (B) particle size distribution profile of silver nanoprisms measured by dynamic light scattering (DLS)

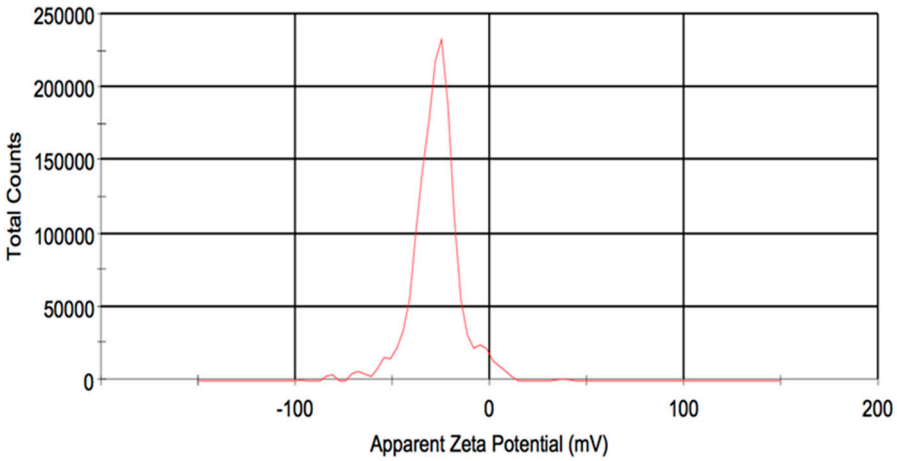

Figure 3: Surface charge distribution of Ag nanoprisms as measured by zeta potential

The elemental analysis of the silver nanoparticles was performed using the energy-dispersive X-ray spectroscope (EDX) equipped on the SEM. The EDX spectrum (not shown) clearly indicated that the prepared samples were pure silver with no other contaminating substances other than a peak corresponding to carbon, which can be attributed to the carbon-coated tape sample substrate, and possibly the PVP capping agent.

3.2. Spectral Shift in the Presence of Hg^{+}

The Ag nanoprisms were used to detect Hg^{2+} based on the blue shift of the maximum absorption wavelength. As shown in Figure 4A, silver nanoprisms in the absence of mercury were characterized by a peak at 665 nm (curve 1), and when Hg^{2+} was added the maximum absorption wavelength blue shifted. The absorption intensity at 665 nm gradually decreased with an increase in the Hg^{2+} content (curves 2–3).

Peer-reviewed version available at Materials 2019, 12, 1533; doi:10.3390/ma12091533

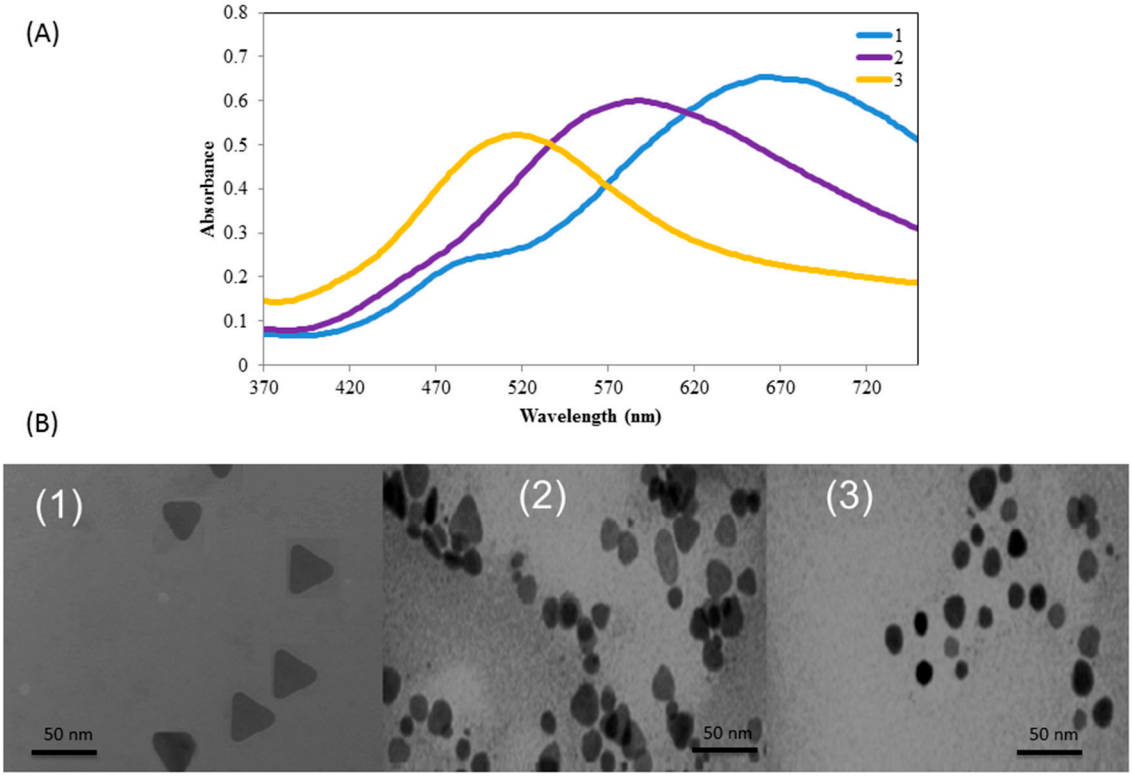

Figure 4: (A) UV-visible spectra and (B) TEM images of the silver nanoprisms in the absence (1) and presence of 2.5 μmole/L (2) and 5 μM (3) Hg^{2+}

In correspondence with the UV-Visible spectra in Figure 4, it was observed that the solution color changed from blue to purple and eventually to yellow at the higher mercury concentrations. Thus, a blue shift was observed in these experiments, which was induced by the presence of Hg^{2+} as noted in other work. Some previous work has attributed the color shift to conformational changes in surface ligands, or aggregation of nanoparticles [13], however in this work there is little evidence for aggregation. Other work has noted the reduction of Hg^{2+} onto the silver in the presence of H_2O_2 [20]. Here, the Hg^{2+} detection appears to also be achieved by forming an Ag/Hg amalgam upon reduction of the mercury species to elemental mercury by silver. In the preparation of Ag nanoprisms, PVP was added to keep them in a stable dispersed state under different environmental conditions. The PVP may act as an electron donor, and the mercury reduction might be supported by the PVP reduction abilities [21]. However, in the presence of the strong oxidizing agent (H_2O_2) used in the preparation of the nanoprisms, the presence of active reducing agents seems uncertain. Therefore the galvanic replacement reaction, whereby a more reactive metal is dissolved and replaced by a less reactive one, seems more likely and this this can occur rapidly at the nanoscale [22].

After interacting with Hg^{2+} ion, the AgNPs solution was centrifuged, washed three times with deionized water to remove the unreacted ions, and subjected to transmission electron microscopy to verify this aspect of the hypothesis. As shown in Figure 4B, the triangle corners gradually disappeared upon interaction with Hg^{2+}. Furthermore, the TEM imaging (Figure 4) shows that the sharp edge and vertex of the original prismatic silver disappeared in the presence of higher Hg^{2+} concentrations. The sharp edges of the nanoprisms are more likely prone to attack and in the presence of Hg^{2+} electrons could be extracted first from the active "corner" areas of the Ag nanoprisms resulting in the shape transformation. Silver or gold with mercury can form bimetallic colloids or amalgam and this also leads to a blue shift of the absorption peak [23, 24]. An elemental analysis of the resultant alloy performed by EDX confirmed the presence of Hg in the colloids (Figure 5). In this work, the reaction of Hg^{2+} with AgNPs appears to cause a combination of a reshaping process

Preprints (www.preprints.org) | NOT PEER-REVIEWED | Posted: 1 April 2019 doi:10.20944/preprints201904.0002.v1

Peer-reviewed version available at Materials 2019, 12, 1533; doi:10.3390/ma12091533

from triangular to spherical, and the formation of amalgam, which is accompanied by a marked optical blue shift of the spherical nanoparticles, as indicated in Figure 4.

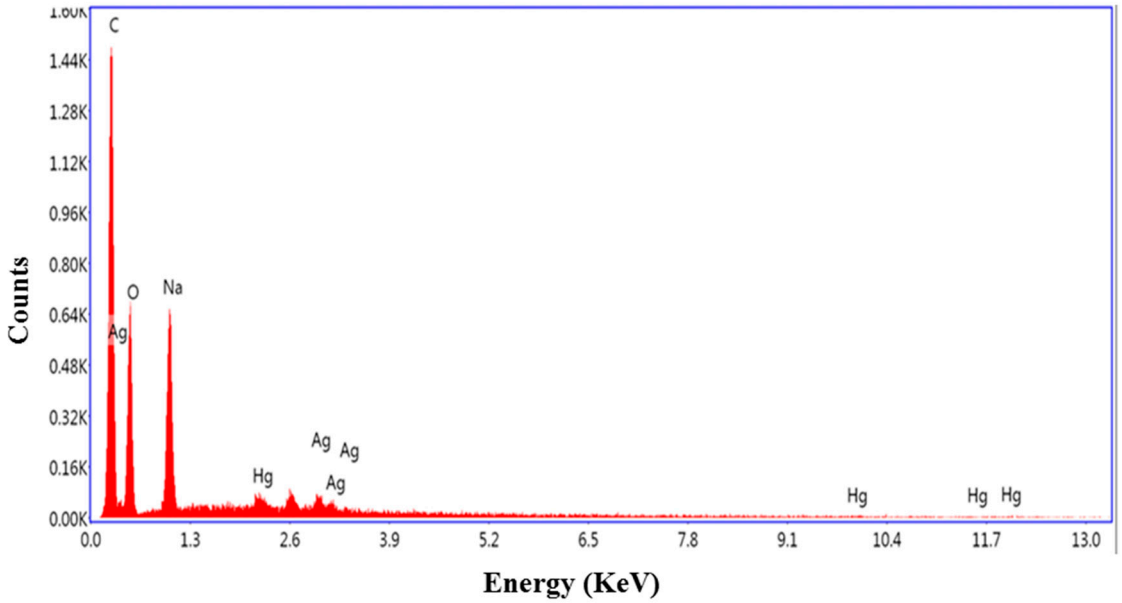

Figure 5: Elemental analysis, performed by energy dispersive X ray spectroscopy (EDX), of nanoparticles after exposure to mercury, indicating the formation of Ag-Hg amalgams.

3.3. Sensitivity and Selectivity

The effect of pH on the proposed detection system was tested in the presence of 5 μmol/L Hg^{2+} and the extent of the absorbance wavelength peak shift was quantified. As shown in Figure 6, the AgNP sensing system was insensitive to pH in the range of 6.5 to 9.79, confirming that the PVP capped silver nanoparticles exhibited excellent stability towards changes in pH [25]. A pH of 7.2 was selected to subsequently determine the sensitivity and selectivity of the system.

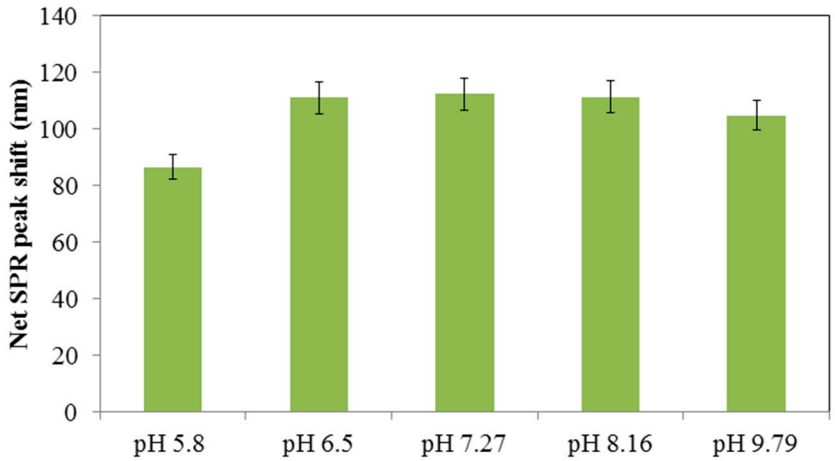

Figure 6: Influence of pH on the extent of the SPR peak shift at 5 μmole/L of Hg^{2+} in 5 mM phosphate buffered saline.

To evaluate the sensitivity of the nanoprisms to Hg^{2+} concentration, the UV−Vis spectra of the silver nanoprism solutions were recorded under the optimized conditions, where different

concentrations of Hg^{2+} were added to the solution and incubated for 30 min. As shown in Figure 4A, upon the addition of increasing concentrations of Hg^{2+}, the SPR band emerged as a blue shift, which was attributed to the morphology changes in the silver nanoprisms. Therefore, the wavelength shift of the surface plasmon band (λ_{max}) of the silver nanoprisms was employed as a quantitative analysis of Hg^{2+}. A typical plot of the wavelength shift versus Hg^{2+} concentrations (0.5−100 μmol/L) is shown in Figure 7. A linear relationship was obtained over the range of 0 to 5 μmol/L with a correlation coefficient of 0.993 (Figure 7B inset). The results suggest that this Ag nanoprism material can be used to detect Hg^{2+} with a detection limit of approximately 0.5 μmol/L (100 μg/L). Although not the most sensitive detection limit ever reported, it compares favorably with the range of 10 nM to 55 μM for other AgNPs reported in one review [8]. Further improvements in sensitivity may be possible with optimization of the concentrations and ratios of AgNPs to sample solutions.

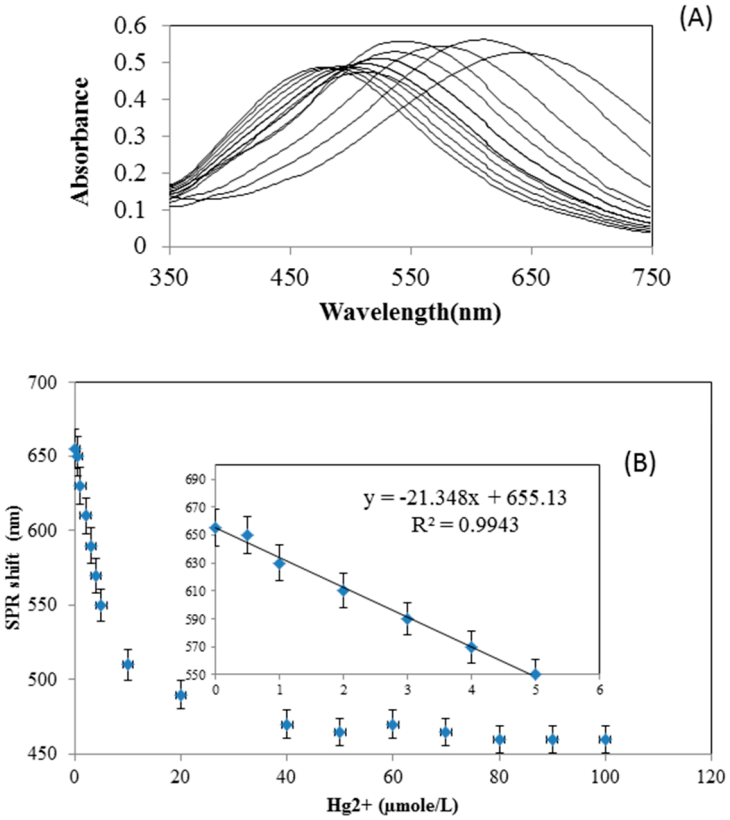

Figure 7: (A) UV−visible absorption spectra of the silver nanoprisms after the addition of different concentrations of Hg^{2+}, with the peak shifting from right to left as Hg^{2+} increases. (B) Wavelength shift of the silver nanoprisms with different concentrations of Hg^{2+} (0−100 μmole/L), where the inset graph shows a linear regression for the range of 0 to 5 μmole/L. The error bars represent the standard deviations based on three independent readings.

To determine and verify the selectivity of the nanoprisms toward Hg^{2+}, the effects of other metal ions including Cd^{2+}, Pb^{2+}, Mg^{2+}, Zn^{2+}, Mn^{2+}, Ba^{2+}, Co^{2+}, Fe^{2+}, Cu^{2+}, K^{+}, and Na^{+} were examined under the optimized conditions. The results demonstrated that only Hg^{2+} caused a significant morphology variation of the silver nanoparticles at 5 μmol/L, as determined by spectroscopy, and a 100- fold excess of the other metal ions had no significant effect on the SPR band shift and the color of the solution under these conditions (Figure 8). These results indicate that the proposed method exhibits a very high selectivity toward Hg^{2+} ions and provides further evidence that the interaction between the AgNPs and Hg^{2+} is primarily driven by a galvanic reaction. The standard reduction potentials for Hg^{2+} and Ag^{+} are 0.85 and 0.80 V, respectively, while those of the other species tested here are all <0.80 V [26]. Therefore of all these metals only Hg^{2+} can thermodynamically be reduced by silver, lending support to the hypothesis that a galvanic reaction is primarily responsible for the nanoprism

Peer-reviewed version available at Materials 2019, 12, 1533; doi:10.3390/ma12091533

morphology changes and SPR blue-shift, rather than aggregation effects alone. There are very few, if any, metals of environmental significance with a reduction potential >0.80 V, suggesting that the silver nanoprisms will always be selective towards mercury, in the absence of any other interfering effects that remain to be discovered.

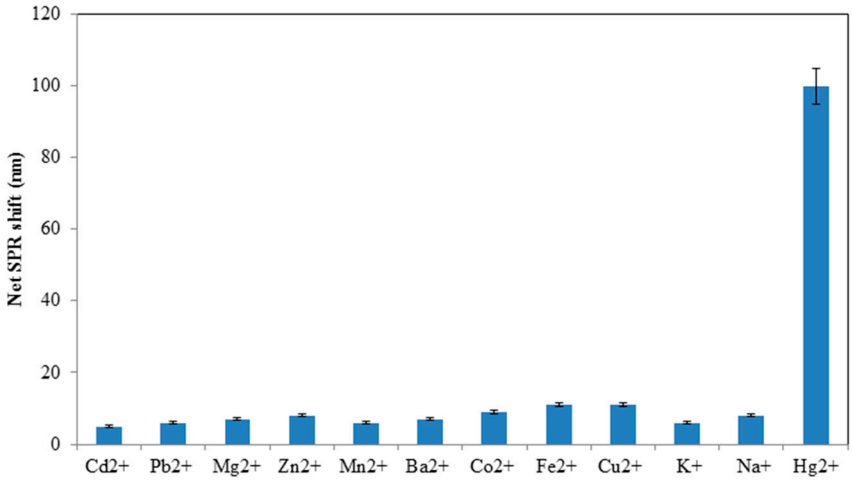

Figure 8: Effect of various metal ions (5 μM) dissolved in 5 mM phosphate buffered saline pH 7.2 on the net SPR shift, showing high selectivity for Hg^{2+}

To further explore the nature of the nanoprism/metal interactions, negative control experiments were performed. Chelating agents are capable of binding to metal ions to form a complex that makes them unavailable to react with the silver nanoparticles. Therefore the metal ion chelator EDTA was used to establish a negative control. The various metal ions and Hg (II) were mixed with 10 mM EDTA and then allowed to interact with the prismatic silver reagent. No color change was noted under these conditions, confirming that the previously measured effects are due to Hg^{2+}, and that chelated ions may not be detectable via this method.

4. Conclusions

The technique developed by this study, using PVP capped prismatic nanosilver, provides a rapid, sensitive and selective detection method for aqueous Hg^{2+} samples and may be potentially suitable for remote field and environmental analysis where more advanced instrumentation is not readily available. The silver in the nanoparticles is believed to form an amalgam with mercury ion through a galvanic reduction process, as identified by the EDX spectrum and the lack of sensitivity to other metal ions. The minimum detection limit for this reagent was found to be approximately 0.5 μmol/L under controlled conditions. The selectivity for Hg^{2+} was evaluated and confirmed through experiments with a variety of other common heavy metals and alkali metals. Using these prismatic silver nanoparticles may offer a useful approach for the detection of mercury (II) in aqueous environmental samples, but additional optimization work is required to lower the detection limit further.

Author Contributions: Conceptualization, F.T. and S.T.; methodology, F.T., S.T., and R.A.; investigation, F.T. and R.A.; resources, W.A.; writing—original draft preparation, F.T. and R.A..; writing—review and editing, S.T., A.Y. and W.A.; supervision, A.Y. and W.A.; project administration, W.A. and S.T.; funding acquisition, W.A.

Funding: This research was funded in part by the Ontario Centres of Excellence Voucher for Innovation and Productivity I program. F. Tanvir was supported by an International Research Support Initiative Program grant offered by Higher Education Commission (HEC) Islamabad, Pakistan.

Conflicts of Interest: The authors declare no conflict of interest. The funders had no role in the design of the study; in the collection, analyses, or interpretation of data; in the writing of the manuscript, or in the decision to publish the results.

References

1. Streets, D. G., Horowitz, H. M., Lu, Z., Levin, L., Thackray, C. P., & Sunderland, E. M. (2019). Global and regional trends in mercury emissions and concentrations, 2010–2015. *Atmospheric Environment*, *201*, 417-427.
2. Zhang, L., Wang, S., Wu, Q., Wang, F., Lin, C. J., Zhang, L., ... & Hao, J. (2016). Mercury transformation and speciation in flue gases from anthropogenic emission sources: a critical review. *Atmospheric chemistry and physics*, *16*(4), 2417-2433.
3. Leopold, K., Foulkes, M., & Worsfold, P. (2010). Methods for the determination and speciation of mercury in natural waters—a review. *Analytica chimica acta*, *663*(2), 127-138.
4. Martín-Yerga, D., González-García, M. B., & Costa-García, A. (2013). Electrochemical determination of mercury: a review. *Talanta*, *116*, 1091-1104.
5. Bui, M. P. N., Brockgreitens, J., Ahmed, S., & Abbas, A. (2016). Dual detection of nitrate and mercury in water using disposable electrochemical sensors. *Biosensors and Bioelectronics*, *85*, 280-286.
6. Wang, Y., Yang, F., & Yang, X. (2010). Colorimetric biosensing of mercury (II) ion using unmodified gold nanoparticle probes and thrombin-binding aptamer. *Biosensors and Bioelectronics*, *25*(8), 1994-1998.
7. Han, K. N., Choi, J. S., & Kwon, J. (2017). Gold nanozyme-based paper chip for colorimetric detection of mercury ions. *Scientific reports*, *7*(1), 2806.
8. Zarlaida, F., & Adlim, M. (2017). Gold and silver nanoparticles and indicator dyes as active agents in colorimetric spot and strip tests for mercury (II) ions: a review. *Microchimica Acta*, *184*(1), 45-58.
9. Farhadi, K., Forough, M., Molaei, R., Hajizadeh, S., & Rafipour, A. (2012). Highly selective Hg2+ colorimetric sensor using green synthesized and unmodified silver nanoparticles. *Sensors and Actuators B: Chemical*, *161*(1), 880-885.
10. Zhan, L., Yang, T., Zhen, S. J., & Huang, C. Z. (2017). Cytosine triphosphate-capped silver nanoparticles as a platform for visual and colorimetric determination of mercury (II) and chromium (III). *Microchimica Acta*, *184*(9), 3171-3178.
11. Jeevika, A., & Shankaran, D. R. (2016). Functionalized silver nanoparticles probe for visual colorimetric sensing of mercury. *Materials Research Bulletin*, *83*, 48-55.
12. Li, L., Gui, L., & Li, W. (2015). A colorimetric silver nanoparticle-based assay for Hg (II) using lysine as a particle-linking reagent. *Microchimica Acta*, *182*(11-12), 1977-1981.
13. Wang, Y., Yang, F., & Yang, X. (2010). Colorimetric detection of mercury (II) ion using unmodified silver nanoparticles and mercury-specific oligonucleotides. *ACS applied materials & interfaces*, *2*(2), 339-342.
14. Alam, A., Ravindran, A., Chandran, P., & Khan, S. S. (2015). Highly selective colorimetric detection and estimation of Hg2+ at nano-molar concentration by silver nanoparticles in the presence of glutathione. *Spectrochimica Acta Part A: Molecular and Biomolecular Spectroscopy*, *137*, 503-508.
15. Manivel, P., & Ilanchelian, M. (2017). Selective and Sensitive Colorimetric Detection of Hg 2+ at Wide pH Range Using Green Synthesized Silver Nanoparticles as Probe. *Journal of Cluster Science*, *28*(3), 1145-1162.
16. Detsri, E. (2016). Novel colorimetric sensor for mercury (II) based on layer-by-layer assembly of unmodified silver triangular nanoplates. *Chinese Chemical Letters*, *27*(10), 1635-1640.
17. Tanvir, F., Yaqub, A., Tanvir, S., & Anderson, W. (2017). Poly-l-arginine coated silver nanoprisms and their anti-bacterial properties. *Nanomaterials*, *7*(10), 296.
18. Panzarasa, G., Just What Is It That Makes Silver Nanoprisms so Different, so Appealing? Journal of Chemical Education, 2015. 92(11): p. 1918-1923.
19. Torres, V., Popa, M., Crespo, D., & Moreno, J. M. C. (2007). Silver nanoprism coatings on optical glass substrates. *Microelectronic Engineering*, *84*(5-8), 1665-1668.
20. Wang, G. L., Zhu, X. Y., Jiao, H. J., Dong, Y. M., & Li, Z. J. (2012). Ultrasensitive and dual functional colorimetric sensors for mercury (II) ions and hydrogen peroxide based on catalytic reduction property of silver nanoparticles. *Biosensors and Bioelectronics*, *31*(1), 337-342.

21. Wu, C., Mosher, B. P., Lyons, K., & Zeng, T. (2010). Reducing ability and mechanism for polyvinylpyrrolidone (PVP) in silver nanoparticles synthesis. *Journal of nanoscience and nanotechnology*, *10*(4), 2342-2347.
22. Wang, Y., Wen, G., Ye, L., Liang, A., & Jiang, Z. (2016). Label-free SERS study of galvanic replacement reaction on silver nanorod surface and its application to detect trace mercury ion. *Scientific reports*, *6*, 19650.
23. Rex, M., Hernandez, F. E., & Campiglia, A. D. (2006). Pushing the limits of mercury sensors with gold nanorods. *Analytical Chemistry*, *78*(2), 445-451.
24. Kamali, K. Z., Pandikumar, A., Jayabal, S., Ramaraj, R., Lim, H. N., Ong, B. H., ... & Huang, N. M. (2016). Amalgamation based optical and colorimetric sensing of mercury (II) ions with silver@ graphene oxide nanocomposite materials. *Microchimica Acta*, *183*(1), 369-377.
25. Badawy, A. M. E., Luxton, T. P., Silva, R. G., Scheckel, K. G., Suidan, M. T., & Tolaymat, T. M. (2010). Impact of environmental conditions (pH, ionic strength, and electrolyte type) on the surface charge and aggregation of silver nanoparticles suspensions. *Environmental science & technology*, *44*(4), 1260-1266.
26. Haynes, W.M., The CRC Handbook of Chemistry and Physics, 97th Edition, in Library Journal. 2017, CRC press/Taylor & Francis, Boca Raton, FL. p. 192-+.